Available online at www.sciencedirect.com
SCIENCE DIRECT®
Journal of Organometallic Chemistry 689 (2004) 2256–2267
Journal of Organometallic Chemistry
www.elsevier.com/locate/jorganchem

Potential inhibitors of DNA topoisomerase II: ruthenium(II) poly-pyridyl and pyridyl-azine complexes

Manish Chandra [a], A.N. Sahay [a], D.S. Pandey [a,*], R.P. Tripathi [b], J.K. Saxena [b], V.J.M. Reddy [b], M. Carmen Puerta [c], Pedro Valerga [c]

[a] *Department of Chemistry, Awadhesh Pratap Singh University, Rewa 486 003 (M.P.), India*
[b] *Medicinal and Biochemistry Division, Central Drug Research Institute, P.B. No.173, Chattar Manzil, Lucknow (U.P.), India*
[c] *Departmento de Ciencia de los Materiales e Ingenieria Metallurgica y Quimica Inorganica, Facultad de Ciencia, Universidad de Cadiz, Apartado – 40, Puerto Real 11510, Spain*

Received 24 January 2004; accepted 26 March 2004

Abstract

In search of new DNA probes a series of new mono and binuclear cationic complexes $[RuH(CO)(PPh_3)_2(L)]^+$ and $[RuH(CO)(PPh_3)_2(\text{-}\mu\text{-}L)RuH(CO)(PPh_3)_2]^{2+}$ [L = pyridine-2-carbaldehyde azine (paa), *p*-phenylene-bis(picoline)aldimine (pbp) and *p*-biphenylene-bis(picoline)aldimine (bbp)] have been synthesized. The reaction products were characterized by microanalyses, spectral (IR, UV–Vis, NMR and ESMS and FAB-MS) and electrochemical studies. Structure of the representative mononuclear complex $[RuH(CO)(PPh_3)_2(paa)]BF_4$ was crystallographically determined. The crystal packing in the complex $[RuH(CO)(PPh_3)_2(paa)]BF_4$ is stabilized by intermolecular π–π stacking resulting into a spiral network. Topoisomerase II inhibitory activity of the complexes and a few other related complexes $[RuH(CO)(PPh_3)_2(L)]^+$ {L = 2,4,6-tris(2-pyridyl)-1,3,5-triazine (tptz) and 2,3-bis(2-pyridyl)-pyrazine (bppz)} have been examined against filarial parasite *Setaria cervi*. Absorption titration experiments provided good support for DNA interaction and binding constants have also been calculated which were found in the range 1.2×10^3–4.01×10^4 M^{-1}.

Keywords: Ruthenium; Poly-pyridyl and pyridyl-azine ligands; Hydride; DNA; Topoisomerase II; π–π interaction

1. Introduction

Ruthenium(II) poly-pyridyl complexes have received considerable recent attention, because of their interesting photo-physical and photo-chemical properties, possible use in photo-chemical molecular devices and as light sensitive probes in biological systems [1a–1d]. In this regard, poly-pyridyl bridging ligands viz. 2,4,6-tris(2-pyridyl)-1,3,5-triazine (tptz) and 2,3-bis(2-pyridyl)-pyrazine (bppz) and other related diimines have drawn special attention. Poly-pyridyl ligands have extensively been used in the synthesis of mono and bi/polynuclear, homo/hetero-metallic complexes possessing interesting spectroscopic, photo-physical and photo-chemical properties [2a–2g]. Although, closely related pyridyl azine ligands like pyridine-2-carbaldehyde azine (paa), *p*-phenylene-bis(picoline)aldimine (pbp) or *p*-biphenylene-bis(picoline)aldimine (bbp) have long been known (Fig. 1), there are only a few reports dealing with their complexes with the metal ions. Further, most of the reports are mainly on the complexes of the first transition series metal ions and molybdenum and iridium [3a–3g].

At the same time, synthesis and characterization of metallo-intercalators based on Ru(II) poly-pyridyl complexes that can probe and target nucleic acids have drawn much attention [4a–4e]. A detailed study of the mode of interaction of the complexes with DNA will

* Corresponding author. Tel./fax: +91-766230684.
E-mail address: dsprewa@yahoo.com (D.S. Pandey).

0022-328X/$ - see front matter © 2004 Elsevier B.V. All rights reserved.
doi:10.1016/j.jorganchem.2004.03.044

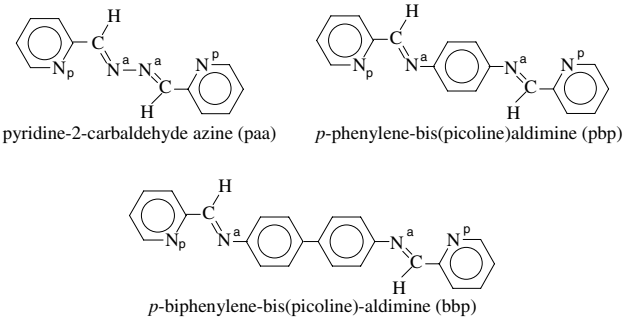

Fig. 1. Diagrammatical representation of ligands used in the synthesis of complexes (paa, pbp, bbp).

lead, not only to new novel chemotherapeutics, but to highly sensitive diagnostic agents too [5a–5l]. It is well documented that, human lymphatic filariasis caused by helminths, *Wuchereria bancrofti* (90% cases) and *Burgia malayi* (10% cases), affects approximately 120 million people, and one billion people are considered to be at the risk of being affected [6]. During past few years, we are working towards identification of novel therapeutic targets. Only recently, DNA topoisomerase II (topo II) of the filarial parasite *S. cervi* have been identified as a target for the development of anti-filarial compounds [7a,7b].

Because of our interests in this area, we have initiated work on designing of metallo-intercalators containing functionalized poly-pyridyl ligands to achieve site-specific DNA recognition. During studies on Ru(II) azine/poly-pyridyl complexes, it was felt that the complexes containing pyridine-2-carbaldehyde (paa), *p*-phenylene-bis(picoline)aldimine (pbp), *p*-biphenylene-bis(picoline)aldimine (bbp), 2,4,6-tris(2-pyridyl)-1,3,5-triazine (tptz) and 2,3-bis(2-pyridyl)-pyrazine (bppz) ligands, may not only accentuate DNA-binding of the ensuing complexes, but facilitate the study of other interesting associated functional aspects too. Although, a number of reports dealing with DNA cleavage and inhibitory activity of ruthenium complexes are available in the literature, the application of hydride complexes in this regard is unusual. In this direction, mono and binuclear Ru(II) hydrido carbonyl complexes $[RuH(CO)(PPh_3)_2(paa)]BF_4$ (**1**), $[RuH(CO)(PPh_3)_2(paa)]PF_6$ (**2**), $[RuH(CO)(PPh_3)_2(pbp)]PF_6$ (**3**), $[RuH(CO)(PPh_3)_2(-\mu\text{-}pbp)RuH(CO)(PPh_3)_2](BF_4)_2$ (**4**), $[RuH(CO)(PPh_3)_2(bbp)RuH(CO)(PPh_3)_2](BF_4)_2$ (**5**) were synthesized. Further, anti-filarial activity of the complexes **1**–**5** and their efficacy as anti-filarial drugs and that of some other related complexes $[RuH(CO)(PPh_3)_2(\eta^2\text{-tptz})]BF_4$ (**6**), $[RuH(CO)(PPh_3)_2(\eta^2\text{-bppz})]BF_4$ (**7**), $[RuH(CO)(PPh_3)_2(\eta^2\text{-bppz})]PF_6$ (**8**) have been examined [12b]. In this paper, we report the studies on the synthesis, spectral, electrochemical and structural characterization and topo II activity of some Ru(II) poly-pyridyl hydrido carbonyl complexes.

2. Experimental

2.1. General

All the reactions were carried out under nitrogen atmosphere and in de-aerated solvents. The solvents were of AR grade and were purified rigorously by standard procedures prior to their use [8]. Triply distilled and deionized water was used for the preparation of various buffers. 2,3-Bis(2-pyridyl)-pyrazine (bppz); 2,4,6-tris(2-pyridyl)-1,3,5-triazine (tptz), ammonium tetrafluoroborate, ammonium hexafluorophosphate, ruthenium(III) chloride hydrate (all Aldrich) and tetrabutylammonium perchlorate (Fluka) were used as received without further purification. Calf thymus (CT) DNA, Supercoiled pBR322 DNA, bovine serum albumin (BSA), ATP, dithiothreitol (DTT), agarose, ethidium bromide, sodium dodecyl sulphate (SDS) and proteinage were procured from Sigma Chemical Co., St. Louis. Topo II from filarial parasite *S. cervi* was partially purified according to the method by Pandeya et al. [7a]. The ligands pyridine-2-carbaldehyde azine (paa), *p*-phenylene-bis(picoline)aldimine (pbp) and *p*-biphenylene-bis(picoline) aldimine (bbp) and the precursor complex $[RuH(CO)Cl(PPh_3)_3]$ were prepared and purified following the literature procedures [9a–9c].

2.2. Physical measurements

Microanalyses of the complexes were obtained from micro-analytical section of the Sophisticated Analytical Instrumentation Facility, Central Drug Research Institute, Lucknow. IR and electronic spectra using quartz cuvette with a path length of 1 cm were recorded on a Shimadzu-8201PC and Shimadzu-UV-1601 spectrophotometers, respectively. ^1H, ^1H–^1H COSY, ^{13}C and ^{31}P NMR spectra were recorded on a Bruker DRX-300 NMR instrument. Electrospray mass spectra were recorded on a Micromass-Quattro-II triple quadrupole mass spectrometer. Samples were introduced into the ESI source through a syringe pump at 0.4 ml h^{-1}. The ESI capillary was 3.5 kV and cone-voltage 25–50 V. Spectra were collected in 4s scans and printouts were averaged spectra of 5–10 scans. FAB mass spectra were recorded on a JEOL SX 102/DA 6000 mass spectrometer using xenon (6 kV and 10 mA) as the FAB gas. The accelerating voltage was 10 kV and the spectra were recorded at room temperature with *m*-nitrobenzyl alcohol as the matrix. Thermal denaturation analyses were conducted on a DU-640 spectrophotometer. Electrochemical data were acquired on a PAR model 273A electrochemistry system at a scan rate of 50 mV s^{-1}. The sample solutions (10^{-3} M) were prepared in purified acetonitrile containing $Et_4^+ClO_4^-$ (0.1 M) as a supporting electrolyte. Solution was deoxygenated by bubbling dinitrogen for about 20 min for each experiment.

Platinum wire working and auxiliary electrodes and an aqueous saturated calomel reference electrode were used in a three-electrode configuration.

2.3. Preparation of the complexes

2.3.1. Preparation of [RuH(CO)(PPh$_3$)$_2$(paa)]BF$_4$ (1)

A suspension of [RuH(CO)Cl(PPh$_3$)$_3$] (955 mg and 1 mmol) in methanol (60 mL) was treated with pyridine-2-carbaldehyde azine (paa) (420 mg and 2 mmol) and the resulting solution was heated under reflux for about 20 h. The precursor complex [RuH(CO)Cl(PPh$_3$)$_3$] slowly dissolved and gave a bright orange solution. It was cooled to room temperature and filtered through celite to remove any solid residue. Saturated solution of NH_4BF_4 in methanol (25 mL) was added to the filtrate, the solution was reduced in volume using a rotatory evaporator to about 25 mL and was left in refrigerator for slow crystallization. Crystalline product appeared in a couple of days. The crystals (complex **1**) were separated by filtration, washed with methanol, diethylether and dried in vaccuo. Yield: 80% (762.4 mg); Anal. Calc. for $BC_{49}F_4H_{41}N_4OP_2Ru$: C, 61.69; H, 4.30; N, 5.87, Found: C, 60.13; H, 4.13; N, 5.67%. ESMS (*m*/*z*): 865.1 Calc. for [RuH(CO)(PPh$_3$)$_2$(*paa*)]$^+$ (864). FAB MS *m*/*z* obs. (Calc.): 864 (864), 600 (602), 572 (572); IR (cm^{-1}, nujol): 2005 ν(Ru–H), 1954 ν(CO), 1625, 1593, 1475, 1434, 1394, 1087, 1055, 950.8, 848, 746, 696 (bands due to *paa*, PPh$_3$, and counter anion BF_4^-); ^{1}H NMR (δ ppm, acetone-d$_6$, 300 MHz, 25 °C): 9.30 (d, 4.8 Hz), 8.94 (t, 2.4 Hz), 8.76 (s), 8.65 (d, 6.8 Hz), 7.99 (d, 3.6 Hz), 7.46 (m, 1H), −10.71 (t, 19.4 Hz); ^{31}P{^{1}H}: 43.28 (s); UV–Vis{CH_2Cl_2; λ_{max}, nm(ε)}: 605(5.0×10^3), 475 (1.98×10^4), 428(3.8×10^4), 390(3.5×10^4), 311(1.68×10^4).

2.3.2. Preparation of [RuH(CO)(PPh$_3$)$_2$(paa)]PF$_6$ (2)

Complex **2** was prepared by the same procedure as described for complex **1** by the reaction of [RuH(CO)Cl(PPh$_3$)$_3$] (477 mg and 0.5 mmol) in methanol (30 mL) with pyridine-2-carbaldehyde azine (paa) (210 mg and 1 mmol). The complex separated as bright yellow needles. Yield: 64% (324 mg); Anal. Calc. for $C_{49}F_6H_{41}N_4OP_3Ru$: C, 58.16; H, 4.05; N, 5.53; Found: C, 58.01; H, 3.92; N, 5.20%. FAB MS *m*/*z* obs. (calc.): 865 (864), 600 (602), 572 (572). IR (cm^{-1}, nujol): 2003 *ν*(Ru–H), 1953.8 *ν*(CO), 1625, 1591, 1477, 1434, 1305, 1091, 997, 840, 775, 746, 696, 516 (bands due to paa, PPh$_3$ and counter anion PF_6^-); ^{1}H NMR (δ ppm, Acetone-d$_6$, 300 MHz, 25 °C): 9.338 (d, 4.9 Hz), 8.96 (t, 2.3 Hz), 8.791 (s), 8.586 (d, 6.7 Hz), 7.983 (d, 3.5 Hz), 7.45 (m, 1H), −10.769 (t, 19 Hz); ^{31}P{^{1}H}: 44.213 (s); UV–Vis{CH_2Cl_2; λ_{max}, nm(ε)}: 591(7.0×10^3), 466(2.2×10^4), 387(3.1×10^4), 290(1.2×10^4).

2.3.3. Preparation of [RuH(CO)(PPh$_3$)$_2$(pbp)]PF$_6$ (3)

Complex **3** was prepared by the same method as described for complex **1** by the reaction of [RuH(CO)Cl(PPh$_3$)$_3$] (477 mg and 0.5 mmol) and *p*-phenylene-bis(picoline)aldimine (pbp) (286 mg and 1 mmol). It was separated as yellow microcrystalline product. Yield: 72% (391.32 mg); Anal. Calc. for $C_{55}F_6H_{45}N_4OP_3Ru$: C, 60.17; H, 4.13; N, 5.15; Found: C, 59.36; H, 4.22; N, 5.46%. FAB MS (*m*/*z*): 939 (Calc. for [RuH(CO)(PPh$_3$)$_2$(pbp)]$^+$) (940). IR (cm^{-1}, nujol): 2002 *ν*(Ru–H), 1946 *ν*(CO), 1627, 1479, 1431, 1396, 1313, 1163, 1159, 1091, 999, 840, 746, 696, 555 (characteristic bands due to pbp, PPh$_3$, and counter anion PF_6^-); ^{1}H NMR (ppm, $CDCl_3$, 300 MHz, 25 °C): 8.92 (d), 8. 67 (s), 8.60 (d, 4.4 Hz), 7.89 (m), 7.62 (t, 4.3 Hz), 7.03 (m) −10.89 (t, 19 Hz Ru–H); ^{13}C{^{1}H}: δ 206 (carbonyl carbon), 166.4, 162.3, 150.3, 150.1, 138.0, 133.8, 130.08, 127.9, 117 ppm (carbons of the pbp ligand); ^{31}P{^{1}H}: 43.21 (s) UV–Vis{CH_2Cl_2; λ_{max}, nm(ε)}: 465(6.1×10^4), 310(1.6×10^4), 295(2.35×10^4).

2.3.4. Preparation of [RuH(CO)(PPh$_3$)$_2$(-μ-pbp)-RuH(CO)(PPh$_3$)$_2$](BF$_4$)$_2$ (4)

Complex **4** was prepared following the above procedure by starting with [RuH(CO)Cl(PPh$_3$)$_3$] (477 mg and 0.5 mmol) and *p*-phenylene-bis(picoline)aldimine (pbp) (118 mg, 0.5 mmol). Yellow brown crystals separated out. Yield 68% (599.40 mg). Anal. Calc. for $B_2C_{92}F_8H_{76}N_4O_2P_4Ru_2$: C, 62.30; H, 4.28; N, 3.16; Found: C, 61.67; H, 4.40; N, 3.44%. IR (cm^{-1}, nujol): 2000 *ν*(Ru–H), 1951 *ν*(CO), 1618, 1581, 1479, 1433, 1389, 1311, 1085, 1029, 750, 840, 746, 698 (characteristic bands due to pbp, PPh$_3$, and counter anion BF_4^-); ^{1}H NMR (δ ppm, $CDCl_3$, 300 MHz, 25 °C): 9.01 (d, 5.4 Hz), 8.70 (s), 8.60 (d, 4.5 Hz), 7.91 (t, 5.8 Hz), 7.62 (t, 6.0 Hz), 7.03 (m) −11.8 (m), Ru–H; ^{13}C{^{1}H}: δ 206 (carbonyl carbon), 164.4, 162.3, 150.3, 149.1, 138.0, 133.8, 130.08, 128.9, 113 ppm (carbons of the pbp ligand); ^{31}P{^{1}H}: δ 47.6 ppm (s); UV–Vis{CH_2Cl_2; λ_{max}, nm(ε)}: 540(8.0×10^3), 410(2.2×10^4), 394(1.1×10^4), 241(1.2×10^4).

2.3.5. Preparation of [RuH(CO)(PPh$_3$)$_2$(-μ-bbp)RuH-(CO)(PPh$_3$)$_2$](BF$_4$)$_2$ (5)

Complex **5** was prepared by the same method as described for complex **1** by treating [RuH(CO)Cl(PPh$_3$)$_3$] (477 mg, 0.5 mmol) in methanol (30 mL) with bbp (181 mg, 0.5 mmol). The complex separated as yellowish red granules. Yield: 60% (554.4 mg). Anal. Calc. for $B_2C_{98}F_8H_{80}N_4O_2P_4Ru_2$: C, 63.63; H, 4.32; N, 3.03; Found: C, 62.51; H, 4.45; N, 3.22%. FAB *m*/*z* obs. (Calc.): 1756 (1757), 1668 (1670), 1410 (1408), 1144 (1146), 1017 (1017), 753 (755), 625 (625), 363(362). IR (cm^{-1}, nujol): 2003 *ν*(Ru–H), 1953.8 *ν*(CO), 1618, 1580, 1481, 1433, 1421, 1389, 1311, 1085, 1029, 750, 840, 746, 698 (characteristic bands due to bbp, PPh$_3$, and counter

anion BF_4^-). ^1H NMR (δ ppm, Acetone-d_6, 300 MHz, 25 °C): 9.10 (d, 5.5 Hz), 8.76 (s), 8.63 (d, 6.5 Hz), 8.43 (t, 5.8 Hz), 7.64 (t, 4.5 Hz), 6.57 (d, 9.0 Hz), −10.78 (m); $^{31}P\{^1H\}$: 44.213 (s); UV–Vis{CH_2Cl_2; λ_{max}, nm(ε)}: 570(1.1×10^4), 415(2.02×10^4), 399(1.6×10^4), 267(9.5×10^3).

2.4. X-ray structure determination of [RuH(CO)-(PPh$_3$)$_2$(paa)]BF$_4$ (1)

Suitable crystals for X-ray crystallographic studies for the complex **1** were obtained from CH_2Cl_2/petroleum ether (60–80) at room temperature over a period of three days. All the pertinent crystallographic data are recorded in Table 1. Intensity data were collected at 293(2)° on Enraf Nonius MACH3 diffractometer using graphite monochromatized Mo Kα radiation ($\lambda = 0.7093$ Å) from plate like dark orange crystal with the dimensions $0.4 \times 0.4 \times 0.1$ mm in the ω–2θ scan mode in the range from 1.62° to 24.91°. Intensities of these reflections were measured periodically to monitor crystal decay.

The structure was solved by direct methods and refined by full-matrix least squares on F^2 (SHELX-97) [10a,10b,10c]. In the final cycles of refinement all the non-H atoms were treated anisotropically. The contribution due to H-atoms attached to carbon atoms was included as fixed contribution. Final value of $R = 0.0423$; $wR_2 = 0.1092$; GOF = 1.068.

Table 1
Crystal data for the complex **1**

Empirical formula	$C_{49}H_{41}B\,F_4N_4O\,P_2Ru$
Formula weight	951.68
Crystal size (mm)	$0.4 \times 0.4 \times 0.1$
Temperature	293(2) K
Wavelength	0.70930 Å
Crystal system, space group	Monoclinic, *P*
a (Å)	14.2461(13)
b (Å)	19.313(2)
c (Å)	16.574(2)
α (°)	90.000(9)
β (°)	92.035(9)
γ (°)	90.000(8)
Volume (Å^3)	4557.2(8)
Z	4
Density (mg m^{-3})	1.387
Absorption coefficient (mm^{-1})	0.472
F(000)	1944
Reflections collected	6915
Unique reflections	6915
Parameters	571
GOF (on F^2)	1.068
R_1 (on F)[a]	0.0423
wR_2	0.1092
Largest difference peak and hole (e Å^{-3})	0.494 and −0.718

[a] $R_1 = \sum[|F_o| - |F_c|]/\sum[|F_o|]$, $wR_2 = \{\sum[w(F_o^2 - F_c^2)^2]/\sum[(F_o^2)]\}^{1/2}$.

2.5. DNA binding and cleavage studies

The concentration of CT DNA was confirmed by using its extinction coefficient at 260 nm (6600 $M^{-1}\,cm^{-1}$) [11a]. After sonication, the solutions of CT DNA in buffer gave a ratio of UV absorbance at A_{260}/A_{280} of ca. 1.87 indicating that the DNA was sufficiently free of protein [11b]. Chloride salts were prepared and fully characterized for binding, cleavage and inhibition studies. ^1H NMR and UV–Vis spectral analyses were used to check the stability of the complexes towards the solvent (water and DMSO) and no change was observed. Buffer A (5 mM Tris–HCl, fs 7.1, 50 mM NaCl) was used for absorption titration and buffer B (50 mM Tris–HCl, pH 7.5, 50 mM KCl) was used for inhibition studies.

Values obtained from absorption titration were used to calculate the intrinsic binding constant K_b [5i] by following equation:

$$[DNA]/(\varepsilon_a - \varepsilon_f) = [DNA]/(\varepsilon_b - \varepsilon_f) + 1/K_b(\varepsilon_b - \varepsilon_f),$$

where ε_a is the extinction coefficient observed for the absorption band at a given DNA concentration, ε_f is the extinction coefficient of the free complex in solution, ε_b is the extinction coefficient of the complex fully bound to the DNA (it is assumed that further DNA addition will not change the absorbance), K_b is the intrinsic binding constant and [DNA] is the DNA concentration in the nucleotides. A plot of $[DNA]/(\varepsilon_a - \varepsilon_f)$ vs. [DNA] gave a slope of $1/(\varepsilon_b - \varepsilon_f)$ and a y intercept equal to $1/K_b(\varepsilon_b - \varepsilon_f)$; K_b is the ratio of slope to y intercept.

2.6. DNA topo II estimation

The reaction catalyzed by DNA topo II was measured as reported by Pandya et al. [7a]. Relaxation of the super coiled DNA pBR322 and separation of the topological isomers of DNA were monitored by gel electrophoresis. For activity measurement, reaction was carried out (10 μl) in a reaction mixture containing buffer B, 10 mM $MgCl_2$; 1 mM ATP; 0.1 mM EDTA; 0.5 mM DTT; 30 μg ml^{-1} BSA and enzyme protein. The reaction was started by incubation at 37 °C for 30 min and stopped by adding 5 μl loading dye. The sample components were separated by electrophoresis on 1% agarose gel in Tris–acetate buffer for 18 h at 20 V. Gels were stained with ethidium bromide (0.5 μg ml^{-1}) visualized and photographed on UVP GDS 7500 UV–transilluminator. The percent relaxation was measured by microdensitometry of gel by Gel base/Gel blot Pro Gel analysis software programme.

2.7. Cleavage studies

The cleavage experiments were carried out with a little modification to the method reported by Mark and

co-workers [7c]. The complexes were mixed with the enzyme and incubated for 10 min at 37 °C after that pBR322 was added and again incubated at 37 °C for 1/2 an hour. It was followed by addition of 2 μl 10% SDS, 2 μl (1 mg ml^{-1}) proteinase K and again incubated for one hour at 37 °C. Reaction was stopped by addition 2 μl of loading dye and loaded into 1% agarose gel. Electrophoresis was carried out as described in DNA topo II estimation.

2.8. T_m determination

T_m analyses were conducted in a DU-640 spectrophotometer by using T_m analysis programme and high performance temperature controller for regulating the temperature of the micro-cuvettes. The temperature range was 40–90 °C and data were recorded at 260 nm. The DNA was prepared in 0.1× SCC buffer, pH 7.2, and metal coordinate compounds were incubated with DNA in a total volume of 300 μl. The change in T_m (ΔT_m) following interaction of DNA with added compounds was calculated by:

$$\Delta T_m = T'_m(\text{DNA} + \text{Compound}) - T_m(\text{DNA}).$$

3. Results and discussion

The cationic mono and binuclear complexes with the general formulation $[RuH(CO)(PPh_3)_2(L)]^+$ and $[RuH(CO)(PPh_3)_2(\mu\text{-}L)RuH(CO)(PPh_3)_2]^{+2}$ (L = paa, pbp or bbp) could be easily prepared in quantitative yield by reaction of $[RuH(CO)Cl(PPh_3)_3]$ with the bridging ligands in methanol in 1:1/1:2 molar ratio (Scheme 1).

The mono and binuclear complexes $[RuH(CO)(PPh_3)_2(paa)]BF_4$ (**1**), $[RuH(CO)(PPh_3)_2\text{-}(paa)]PF_6$ (**2**), $[RuH(CO)(PPh_3)_2(pbp)]PF_6$ (**3**), $[RuH(CO)(PPh_3)_2(\mu\text{-}pbp)RuH(CO)(PPh_3)_2](BF_4)_2$ (**4**), $[RuH(CO)(PPh_3)_2\text{-}(\mu\text{-}bbp)RuH(CO)(PPh_3)_2](BF_4)_2$ (**5**) are bright yellow to golden orange, air-stable, non-hygroscopic shiny crystalline solids. These are sparingly soluble in dichloromethane, chloroform, methanol and ethanol, highly soluble in acetone, acetonitrile, dimethylsulfoxide, dimethylformamide and insoluble in benzene, petroleum ether and diethylether.

Carbon, hydrogen and nitrogen analyses of all the complexes conformed well to their respective formulations. Further information about composition of the complexes has also been obtained from ESMS and FAB mass spectrometry. Presence of the different peaks and overall fragmentation pattern (recorded in Section 2) in the FAB mass spectra of the respective complexes conformed well and strongly supported formulation of the complexes.

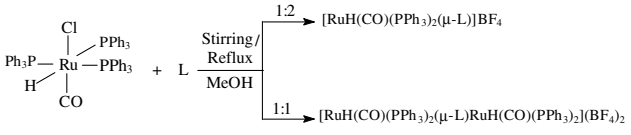

Scheme 1.

Infrared spectra of the complexes exhibited characteristic bands due to coordinated ligands paa, pbp and bbp, PPh_3, CO, hydride group and counter anions in the respective complexes. The ν_{C-N} bands of the pyridyl ring in the complexes shifted towards lower wave numbers and appeared around 1595 cm^{-1} as compared to that in the free ligand (~1640 cm^{-1}). The band associated with pyridyl ring breathing mode appeared at about 1020 cm^{-1}. The shift in the position of ν_{C-N} and pyridine ring breathing mode suggested co-ordination of the ligands through pyridyl and diazine nitrogen with the metal ion. Interestingly, the position of ν(C≡O) and ν(Ru–H) bands shifted toward higher and lower frequencies, respectively, indicating a decrease in the metal to carbonyl carbon interaction. Broad bands in the region 1145 and 845 cm^{-1} have been assigned to counter anions BF_4^- and PF_6^-, respectively.

The ^{1}H NMR spectra of the complexes **1** and **2** (recorded in Section 2) displayed distinct signals at δ 9.30 (d, 4.8 Hz), 8.94 (t, 2.4 Hz), 8.76 (s), 8.65 (d, 6.8 Hz), 7.99 (d, 3.6 Hz), 7.466 (m, 1H) ppm which can be assigned to pyridyl ring and N=CH protons of the ligand paa [12]. The aromatic protons of PPh_3 resonated around δ 7.27–7.33 ppm (as a broad multiplet) and the hydride proton as a triplet in the high field side at −10.713 (t, 19.4 Hz). The protons associated with the bonded ligand paa exhibited downfield shift with respect to those in the free ligand upon coordination with the metal center. $^{13}C\{^1H\}$ NMR spectra of the complex **1** followed the same trends observed in the ^{1}H NMR spectra. The paa carbons resonated at δ 208.00 (*C*≡O), 167.8 (N=*C*H) 157.1; 140.8; 133.3; 131.0–128.24 (pyridyl carbons and aromatic carbons of PPh_3). ^{1}H NMR spectra of the complex **3** also exhibited signals in the same region as that observed for the complex **1** with the additional resonances at 6.4 ppm assigned to C_6H_4 protons of the pbp ligand. The spectrum of the binuclear complex $[RuH(CO)(PPh_3)_2(\mu\text{-}pbp)RuH(CO)(PPh_3)_2](BF_4)_2$ (**4**), displayed signals at δ 9.01 (d, 5.4 Hz), 8.70 (s), 8.60 (d, 4.5 Hz), 7.91 (t, 5.8 Hz), 7.62 (t, 6.0 Hz) corresponding to pyridyl protons, δ 8.36 ppm corresponding to N=CH proton and 7.03 ppm (m) corresponding to C_6H_4 protons of the pbp. The pbp protons exhibited a downfield shift with respect to those in the free ligand. Presence of only five signals in the ^{1}H NMR corresponding to pbp ligand strongly suggested coordination of both the pyridyl and diazine moieties of the ligand bis-chelating two $[RuH(CO)(PPh_3)_2]$. It is in good agreement for a symmetrically bridged complex in which two Ru(II) centers are bridged by the ligand pbp.

The aromatic protons of PPh_3 ligand resonated in its characteristic region at ~7.91–7.62 ppm with the pyridyl protons of the ligand pbp. The $^{13}C\{^1H\}$ spectrum of the complex **4** in $CDCl_3$ exhibited resonance δ 206 (carbonyl carbon), 164.4, 162.3, 150.3, 149.1, 138.0, 133.8, 130.08, 128.9, 113 ppm (carbons of the pbp ligand). It is in good agreement with the conclusions drawn from ^1H NMR spectral studies. The ^1H NMR spectra of the complex **5** showed resonances corresponding to pyridyl and aromatic protons of the ligand bbp and PPh_3 at δ 9.10 (d), 8.76 (s), 8.63 (d), 8.43 (t), 7.64 (t), 6.57 (d) ppm. The position and integrated intensity of the different signals suggested binuclear nature of the complex.

The metal bound hydride protons in the ^1H NMR spectra of complexes **1**–**5** resonated in the high field side around −10 ppm (cf. Section 2). The presence of a triplet or a multiplet in complexes **4** and **5** corresponding to metal bound hydride proton suggested hydride group to be coupled with two equivalent ^{31}P nuclei [13]. The $^{31}P\{^1H\}$ NMR spectra of all the complexes (**1**–**5**) displayed sharp signals around δ 43.5 (recorded in Section 2) indicating equivalence of both the triphenylphosphine ligands in the *trans* position.

Interaction of the filled orbitals of proper symmetry on d^6 Ru(II), with the low lying π^* orbital of the ligands (tptz, bppz or bptz) should show MLCT transition ($t_{2g} \rightarrow \pi^*$) in the electronic spectra of these complexes, with the transition energy varying with nature of the ligands acting as a π acceptor. Our assignments of the bands are based on the same trends as observed in the similar Ru(II) polyazine complexes [13b]. These display $\pi \rightarrow \pi^*$ ligand transition bands in the UV region followed by MLCT band in the visible region. MLCT bands of the complex **1** appeared at about 591, 369, 311 nm, assigned on the basis of intensity and position of the lowest energy absorption [14]. Though, the band at 369 nm may be of MLCT character, but the possibility of σ bond-to-ligand charge transfer (SBLCT) can also not be ruled out [15]. The high-energy band has been assigned to intra-ligand $\pi \rightarrow \pi^*$ transition or π (phenyl) to π^* (phenyl) transitions [16]. The mononuclear ruthenium complex **3** displayed bands at 465, 310 and 295 nm. The low energy band at 465 nm has been assigned to Ru pbp CT transition while the one at 310 nm to intra-ligand $\pi \rightarrow \pi^*$ transition. It was further observed that, in the electronic spectra of the binuclear complex **4**, the Ru → pbp CT transition band appeared at 540 nm while the band associated with intra-ligand transitions are observable at 394 nm. The red shift in the position of Ru → pbp CT transition towards lower energy in the binuclear complex **4**, may be due to stabilization of pbp π^* orbital upon coordination of the second metal center. In general, bridging results in stabilization of the π^* level of the bridging ligand leading to enhanced π–π^* overlap [17]. This effect lowers the HOMO–LUMO energy gap which, in turn, results in a shift of MLCT bands in the binuclear complexes towards lower energy. The stabilization of the pbp π^* also lead to a red shift of the ligand based $\pi \rightarrow \pi^*$ transitions. These observations are consistent with other reports [2f].

Table 2
Selected bond lengths (Å) bond angles (°) and torsion angles (°)

Ru(1)–P(1)	2.3619(11)
Ru(1)–P(2)	2.3643(10)
Ru(1)–N(1)	2.178(3)
Ru(1)–N(2)	2.169(3)
Ru(1)–C(51)	1.848(4)
Ru(1)–H(5)	1.317
P(1)–Ru(1)–P(2)	164.55(4)
P(1)–Ru(1)–N(1)	94.22(9)
P(1)–Ru(1)–N(2)	90.69(9)
P(1)–Ru(1)–H(5)	83.50
P(2)–Ru(1)–H(5)	81.22
P(1)–Ru(1)–C(51)	88.54(13)
P(2)–Ru(1)–C(51)	88.71(13)
P(2)–Ru(1)–N(1)	101.23(9)
P(2)–Ru(1)–N(2)	92.89(9)
N(1)–Ru(1)–N(2)	75.00(12)
N(1)–Ru(1)–C(51)	101.81(15)
N(2)–Ru(1)–C(51)	176.66(15)
N(1)–Ru(1)–H(51)	169.93
N(2)–Ru(1)–H(51)	95.18
C(51)–Ru(1)–H(5)	87.96
C(6)–N(2)–N(3)–C(7)	174.8(4)
N(1)–C(5)–C(6)–N(2)	−2.4(6)
N(3)–C(7)–C(8)–N(4)	5.7(7)
C(5)–C(6)–N(2)–N(3)	−177.7(3)
C(8)–C(7)–N(3)–N(2)	−177.1(3)

Cyclic voltammogram of the complexes **1**, **3** and **4**, were recorded in previously purified acetonitrile and the data is summarized in (Table 4). On the anodic potential window (0 to +2 V vs. SCE) mononuclear complexes **1** and **3** (Fig. 2) exhibited single irreversible and reversible peaks attributed to metal-based oxidation Ru(II/III) at potential 1.38 and 1.17 V, respectively, whereas on the cathodic potential window (0 to −2 V vs. SCE) these complexes exhibited two and three ligand-based reduction couple. Reduction potential of mononuclear complexes $Ru^{II}H(CO)(PPh_3)_2(paa)]^+$ and $Ru^{II}H(CO)(PPh_3)_2(pbp)]^+$ move anodically in order of L = paa < pbp this reflects the lowering of LUMO energy of the ligand. Ligand-based reduction peaks in the complexes were shifted 0.5–0.7 V more positive with respect to those of free ligands.

In the binuclear complex **4**, the metal-centered oxidation occurs at two distinct potentials. The first peak appears at almost the same potential 1.21 V with a small shift with respect to mononuclear complexes whereas the second oxidation process appears at slightly more positive potential 1.32 V. The latter is ascribed to the second Ru ion oxidation. The splitting of the metal-centered oxidation with positive shift compared to that in the mononuclear complexes is a common feature for

Table 3
C–H···F and π–π stacking interaction distances

D–H···A	*d*(D–H)	*d*(H···A)	*d*(D···A)	∠(DHA)
C(1)–H(1)···F(2)[b]	0.93	2.48	3.400(6)	170.2
C(11)–H(11)···F(4)[c]	0.93	2.53	3.366(7)	149.8
C(29)–H(29)···F(4)[a]	0.93	2.48	3.399(8)	170.1

[a] x, y, z.
[b] $x-1/2, -y+1/2, z+1/2$.
[c] $x-1/2, -y+1/2, z-1/2$.

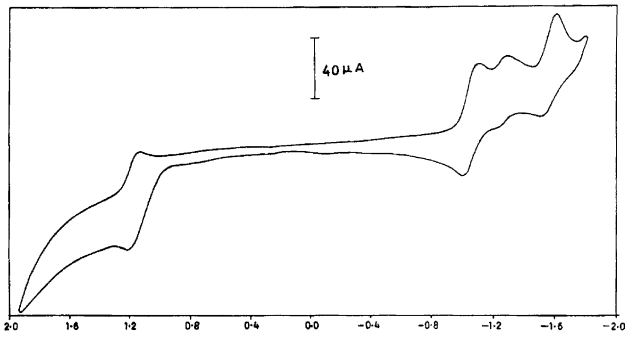

Fig. 2. Cyclic voltammogramm for complex **3**.

all the binuclear complexes and also supports metal–metal interaction through the bridging ligands [18a–18b].

3.1. Single crystal X-ray structure of the complex [RuH(CO)(PPh$_3$)$_2$(paa)]BF$_4$

Structure of the complex **1** has been confirmed by single crystal X-ray diffraction analysis. Details about data collection, reduction and structure solution are recorded in Table 1. An ORTEP [10d] view of the complex cation along with the atom numbering is shown in Fig. 3. Selected bond lengths, bond angles and torsion angles are recorded in Table 2. Coordination geometry about the Ru(II) center is distorted octahedron formed by the atoms N(1), N(2), C(51) and H(5) occupying the equatorial plane and the P donor atoms of the phosphine ligands lie in axial positions. The N(1)–Ru(1)–N(2) angle of 75.00(12)° suggested inward bending of the coordinated pyridyl group. The smaller value of N(1)–Ru(1)–N(2) bite angle 75.00(12)° as compared to the ideal value of 90° is probably the source of observed distortion. The triphenylphosphine ligands lie in *trans* position as indicated by the P(1)–Ru(1)–P(2) angle of 164.55(4)°. The Ru(1)–P(1) and Ru(1)–P(2) distances are 2.3619(11) and 2.3643(10) Å, respectively. These are essentially equivalent and comparable to those in the related complexes [19]. The Ru(1)–C(51) bond length is 1.848(4) Å, which is normal for Ru(II) carbonyls [20a,20b] The Ru(1)–H(5) distance in the complex cation is 1.317 Å. It is shorter than those found in [RuH(H$_2$O)(CO)$_2$(PPh$_3$)$_2$]$^+$ (1.7 Å), [RuHCl(PPh$_3$)$_3$] (1.7 Å), and in other related systems [21a–21c].

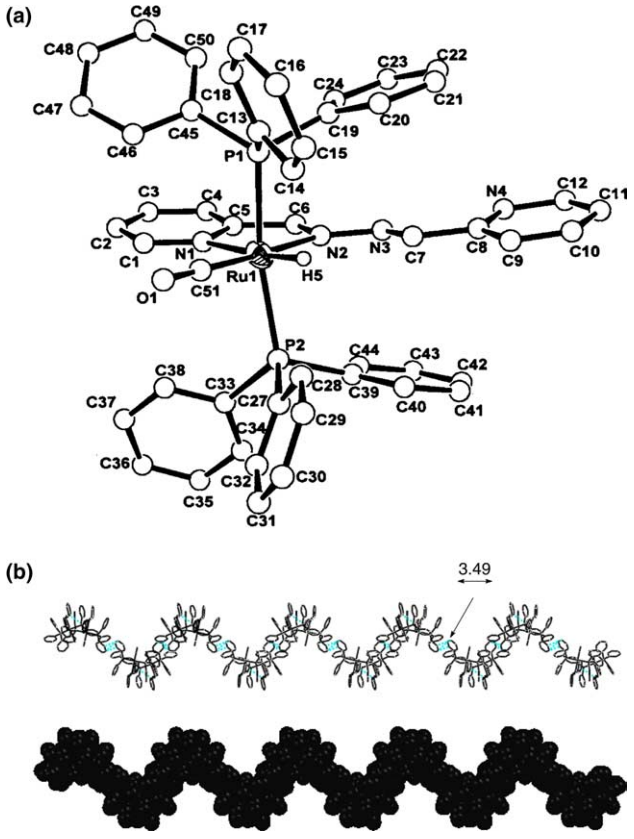

Fig. 3. (a) ORTEP view of complex cation for complex **1**. (b) I. Helical motif obtained by π–π stacking intermolecular interaction. (Hydrogen atom have been omitted for clarity.) and II. Space fill diagram.

The ligand paa is almost planar and the C(6)–N(2)–N(3)–C(7) torsion angle is 174.8(4)°. The Ru(1) to pyridyl N(1) bond length is 2.178(3) Å and it is slightly larger than the Ru(1) to coordinated azine nitrogen N(2) [2.169(3) Å]. These are comparable to those observed in other Ru(II) amine complexes, poly-pyridyl complexes and closely related hydrido carbonyl complex [RuH(CO)(PPh$_3$)$_2$(η^2-tptz)]BF$_4$ [22a–22f]. The N(2)–N(3) bond distance is 1.413(4) Å, it can be defined as single bond and it is comparable with N–N bond length in hydrazine (1.47) Å. The C=N bond lengths C(6)–N(2) and C(7)–N(3) are essentially equal and are 1.278(5) and 1.257(5) Å, respectively, and can be considered to have double bond character.

Weak interaction studies were made by computational programme PLUTON [10e]. The crystal packing in the complex **1** revealed intermolecular C–H···F and intermolecular and intramolecular π–π interaction. Relevant interaction distances are summarized in Table 3. The importance of π–π stacking interactions between aromatic rings has been widely recognized in intercalation of drugs into DNA [23]. Similar aromatic interactions were observed in biological systems, which lie within 3.4–3.5 Å distance [23c]. In complex **1**, both inter and intramolecular (C1–C46) type of π–π interactions has been found with the interaction distances of 3.491

Table 4
Electrochemical data for mono and binuclear Ru(II) complexes in acetonitrile solution at (rt), scan rate 50 mV s^{-1}

S. No.	Complex	$E_{(1/2)}$				
		Oxidation		Reduction		
		I	II	I	II	III
1.	$[RuH(CO)(PPh_3)_2(paa)]BF_4$ (**1**)	1.38 (irr)	–	−0.97 (70)	−1.61 (90)	–
2.	$[RuH(CO)(PPh_3)_2(pbp)]PF_6$ (**3**)	1.17 (60)	–	−1.03 (80)	−1.27 (40)	−1.55 (90)
3.	$[RuH(CO)(PPh_3)_2(\text{-}\mu\text{-pbp})RuH(CO)(PPh_3)_2](BF_4)_2$ (**4**)	1.21 (72)	1.32 (irr)	−1.04 (80)	−1.19 (30)	−1.63 (irr)

$E_{(1/2)} = 0.5(E_{pa} + E_{pc})$, where E_{pa} and E_{pc} are the anodic and cathodic potential, respectively, the value of ΔE_p in (mV is given in parentheses), $\Delta E_p = E_{pa} - E_{pc}$, irr = irreversible.

and 3.211 Å, respectively. Intermolecular π–π stacking interaction (distance 3.49 Å) results in a single helical motif (Figs. 3(b) I and II).

3.2. Thermal denaturation

In general unwinding of DNA is accompanied by lowering in melting temperature (T_m), the temperature at which a DNA double strand unwinds to two single strands. Metal ions which interact through the phosphate groups of the DNA lead to an increase in the melting temperature (T_m), while those interacting through both the phosphate group and nitrogen bases lead to a decrease in the value of melting temperature (T_m) [24]. In the present study, we found that there is insignificant change of 4 °C (±2.0) in the T_m value, which is of least information but supports for intercalative mode of interaction.

3.3. DNA binding

It is well established that, intercalation is not restricted to only completely flat or square planar complexes, but partial intercalation is possible with the ligands coordinated to octahedral metal centers [25a]. Such types of complexes bind to DNA by two non-covalent modes. One is ascribed as an intercalative interaction in the major groove, and the other to groove bound interaction in the minor groove of the helix [25b,25c]. It is essential to mention here that molecular geometry of the complex **1** (obtained from the single crystal data) is exhibiting a plane made up of uncoordinated pyridyl ring and azine nitrogen. The same type of structure is obtained in the complex **6** also where uncoordinated tptz pyridyl and triazine rings are planar. The possibility of partial intercalation of these complexes with the nucleotides can not be ruled out. It has been shown that the Ru(II) poly-pyridyl complexes having octahedral geometry interact with the DNA non-covalently through any of these modes: (i) electrostatically, (ii) hydrophobic interactions of the ligands with the minor groove of the DNA and (iii) by partial intercalation of the uncoordinated planar part of the ligand in mononuclear complexes with the DNA major groove [25d]. The interaction results in an ordered stacking of the bound species between base pairs. The intercalating surface is sandwiched tightly between the aromatic heterocyclic base pairs and stabilized electronically in the helix by π-stacking and dipole–dipole interactions.

Ru(II) complexes used in the present study are octahedral in which the coordination geometry is completed by the carbonyl group, hydride group, pyridyl and azine nitrogen from the ligands (paa, pbp, bbp, bppz, tptz) alongwith the two PPh_3 groups lying *trans* to each other. If we examine the single crystal X-ray structure of the complex **1**, it is evident that planar portion may get stacked between the base pairs of the DNA major groove. However, bulky PPh_3 groups that are trans disposed to each other may interact with the sugar. Such interaction is not possible in the binuclear complexes **4** or **5** due to their non-planar structures. Further due to an increase in the number of bulky PPh_3 groups in these complexes, the possibilities of intercalative stacking by the complexes have been ruled out. It therefore favours the interaction of polynucleotide through a surface bound interaction in the minor groove.

Unwinding of the DNA helix is accompanied by a decrease in the intensity of the absorbance [24a–24c]. Binding of these complexes have successfully been monitored by absorption titration and summarized in preceding section. The ruthenium(II) complexes exhibited the presence of isobestic points, hypochromicity and red shift in the position of absorption maxima with increasing DNA concentration. Hypochromic shifts of 6% and bathochromic shift of upto 4.5 nm were observed. The representative UV–Vis spectra of complexes **3** and **6** are shown in Figs. 4(a) and (b).Complexes under study exhibited hypochromic and bathochromic shift in the position of bands upon addition CT DNA. The calculated values of K_b for the complexes at 20 μM were found to be 3.4×10^4 (**1**), 8.5×10^3 (**2**), 4.25×10^3 (**3**), 1.2×10^3 (**4**), 4.01×10^4 (**6**), 1.7×10^4 (**7**), 1.1×10^4 (**8**). The K_b values obtained for complex **1** and **6** are highest and close to the previously reported Ru(II) complexes [25c]. The trend in the binding constant value

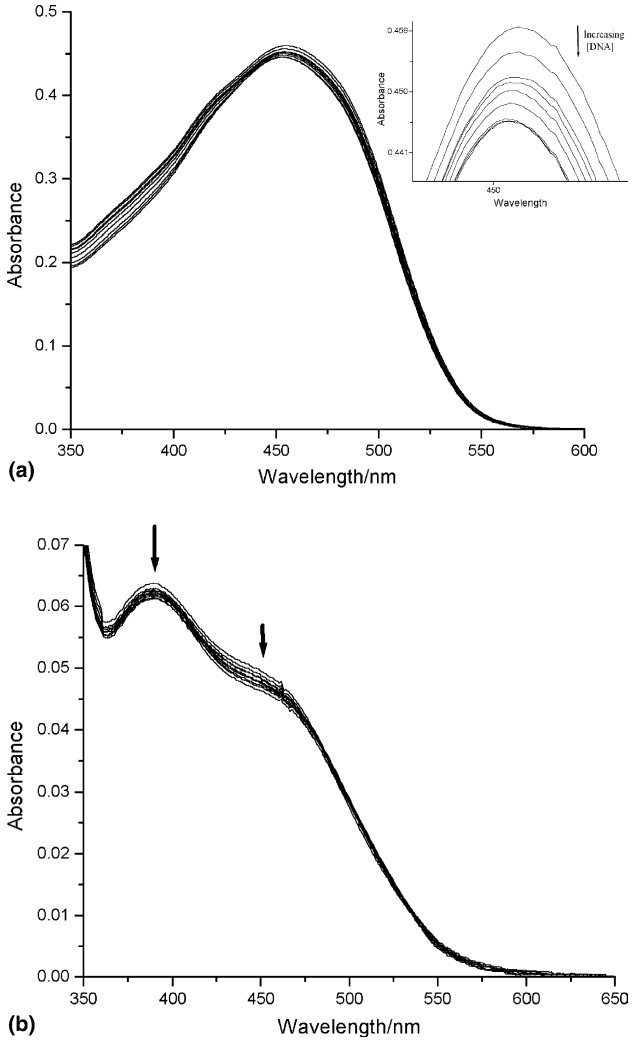

Fig. 4. Absorption spectra of the complexes **3** (a) and **6** (b) in buffer A in the presence of increasing amount of CT (complex concentration 10^{-5} M and CT DNA in buffer, 0–280 μM for complex **3** and 0–320 μM for complex **6**).

corroborated well with conclusions drawn from inhibition data of topo II activity.

An experiment was carried out to support DNA cleavage by the synthesized complexes. It has been shown that topo II is an essential enzyme, which displays an important role in DNA replication, repair and transcription. Complexes that block the overall catalytic activity of topo II can be divided into two classes. First category includes topo II poisons that trap the topo II–DNA cleavage complex, generating high level of DNA breaks. The second category includes topo II inhibitors, which inhibit the overall catalytic activities without inducing DNA breaks. The cleavage experiments were carried out following with a little modification to the method reported by Mark and co-workers [7c]. The ability of these complexes to cause drug induced stabilization of DNA–topo II complex was studied.

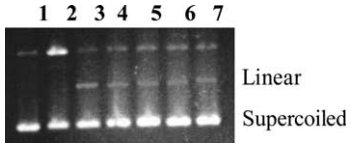

Fig. 5. The cleavage reaction was conducted by incubating pBR322DNA with topo II. Lane 1 pBR322 DNA alone, lane 2 enzyme + DNA, lane 3 complex **1**, lane 4 complex **2**, lane 5 complex **3**, lane 6 complex **6** and lane 7 complex **7**.

Smearing of DNA by complexes **1**–**3**, **6**, and **7** (Fig. 5) supports the cleavage of DNA in presence of complexes. The formation of enzyme–drug–DNA complex can be seen from the appearance of linear DNA which results from DNA strand breaks caused by dissociation of the topo II homo-dimer by SDS. Thus the poly-pyridyl Ru(II) hydrido carbonyl complexes under study could be taken as both topo II inhibitor as well as cleaving agent.

Further interaction behaviour is well supported by the inhibitory effect of metal complexes on DNA topo II activity of filarial parasite *S. cervi* (Figs. 6(a) and (b)). The enzyme was incubated with metal complexes for 10 min at 37 °C and reaction was started by the addition of pBR322 DNA. Enzyme inhibitory activity of complex **1** and **6** were found to be 90% and 95% while, the complexes **2**–**4**, **7** and **8** showed 75%, 80%, 75%, 65% and 55% inhibitory activity at 10 μg per reaction mixture concentration (Table 5). It is clear from the available data that mononuclear complexes are exhibiting higher activity in comparison to binuclear systems. This may result from structural changes discussed above. The ligands being used in the present study contain both the

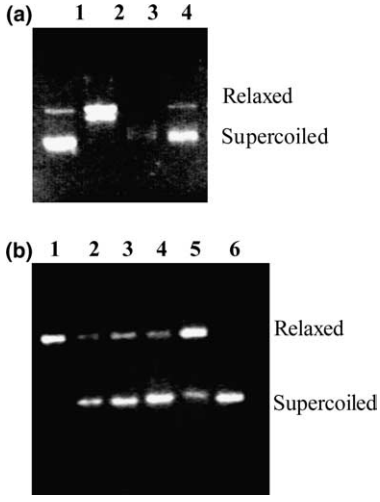

Fig. 6. (a) DNA topisomerase II activity of *S. cervi* of a filarial parasite and effect of metal complexes on the enzyme activity. Lane 1, pBR322DNA alone; lane 2, *S. cervi* enzyme; lane 3, complex **1**; lane 4, complex **3**. (b) Lane 1, *S. cervi* enzyme; lane 2, complex **4**; lane 3, complex **2**; lane 4, complex **7**; lane 5, complex **8**; lane 6, complex **6**.

Table 5
Effect of Ru(II) hydrido carbonyl complexes on DNA topo II activity of *S. cervi*

S. No.	Complex No.	Concentration of complex (μM)	% inhibition
1.	DNA topo II enzyme	–	Nil
2.	**1**	0.105	90
3.	**2**	0.099	75
4.	**3**	0.092	80
5.	**4**	0.056	75
6.	**6**	0.094	95
7.	**7**	0.102	65
8.	**8**	0.096	55

Setaria cervi with enzyme was incubated with the compounds 10 min. at 37 °C. The reaction was started by addition of pBR322 DNA.

pyridyl and the azine type of nitrogen donor atoms. It is observed that the inhibitory activity is dependent upon number of coordinated and uncoordinated donor nitrogen atoms. In the complex **6**, there are six-pyridyl nitrogen atoms out of which, only two are involved in coordination with the metal center and other four nitrogen atoms are uncoordinated. It exhibited maximum inhibition activity (95%). Similarly, in complexes **7** and **8** there are four pyridyl nitrogen atoms but only two of the pyridyl nitrogen atoms are uncoordinated showing 65% and 55% inhibition. It therefore appears that the number of uncoordinated N-atom decides the inhibition activity, the higher the number, higher the activity. Complexes **1**–**4** have both pyridyl and azine nitrogen atoms in it and each of them have only four nitrogen atoms. In the mononuclear complexes **1**–**3**, out of four nitrogen atoms one of the pyridyl and an azine nitrogen atom are involved in coordination with the metal center and other two are uncoordinated. They exhibited inhibitory activity in the range 75–90%, where as, the binuclear complex **4** in which all the four nitrogen atoms are coordinated, showed very poor activity. The inhibitory activity of binuclear complex **5** is the least and it is not discussed here.

In the present work, we have prepared and characterized some mono and binuclear Ru(II) pyridyl-azine complexes. Molecular structure of the representative mononuclear complex $[RuH(CO)(PPh_3)_2(paa)]BF_4$ have been determined by single crystal X-ray studies. Antifilarial activity of the complexes has been studied. The possible efficacy of some complexes $[RuH(CO)(PPh_3)_2(paa)]BF_4$. $[RuH(CO)(PPh_3)_2(paa)]PF_6$ $[RuH(CO)(PPh_3)_2(pbp)]PF_6$, $[RuH(CO)(PPh_3)_2(-\mu\text{-}pbp)RuH(CO)(PPh_3)_2](BF_4)_2$, $[RuH(CO)(PPh_3)_2(-\mu\text{-}bbp)RuH(CO)–(PPh_3)_2](BF_4)_2$, $[RuH(CO)(PPh_3)_2(\eta^2\text{-}tptz)]BF_4$, $[RuH(CO)(PPh_3)_2(\eta^2\text{-}bppz)]BF_4$ and $[RuH(CO)(PPh_3)_2(\eta^2\text{-}bppz)]PF_6$ as anti-filarial drugs has been examined. These complexes are inhibitors of topo II as well as cleaving agent. These studies suggest that the activity or the inhibition towards filarial parasite enzyme is dependent upon: (i) number and type (pyridyl or azine) of coordinated and uncoordinated nitrogen atoms and (ii) mononuclear and binuclear nature of complexes. Finally results obtained from absorption titration and gel electrophoresis experiment suggest these complexes bind to DNA with moderate strength most probably by an intercalative mode.

4. Supporting information available

Crystallographic data for the structural analysis in CIF format have been deposited to CCDC and the deposition code is 229574.

Acknowledgements

Thanks are due to University Grants Commission, New Delhi for providing financial assistance (F-12-21/97). M.C. and A.N.S acknowledge CSIR, New Delhi for awarding SRF and SRA, respectively. Thanks are also due, to RSIC, Central Drug Research Institute, Lucknow, for providing analytical and spectral facilities, National Diffraction Facility, X-ray Division, IIT Mumbai for single crystal data collection and the Head, Department of Chemistry, Awadhesh Pratap Singh University, Rewa for extending laboratory facilities. Special thanks are due to Prof. U.C. Agarwala, Department of Chemistry, Indian Institute of Technology, Kanpur and Prof. P. Mathur, Department of Chemistry, Indian Institute of Technology, Mumbai for their kind help and encouragement.

References

[1] (a) K. Kalyanasundaram, M. Gratzel, Photosensitization and Photocatalysis using Inorganic and Organometallic Compounds, Kluwer Academic, Dordrecht, 1993;
(b) A. Juris, V. Balzani, F. Barigelletti, S. Campagna, P. Belser, A. Von Zelewsky, Coord. Chem. Rev. 84 (1988) 85;
(c) T.J. Meyer, Pure Appl. Chem. 58 (1986) 1193;
(d) N.H. Dam Rauer, G. Cerullo, A. Yeh, T.R. Boussie, C.V. Shank, J.K. McCusker, Science 275 (1997) 54.
[2] (a) N. Gupta, N. Grover, G.A. Neyhart, P. Singh, H.H. Thorp, Inorg. Chem. 32 (1993) 310;
(b) E. Brauns, W. Sumner, J.A. Clark, S.M. Molnar, Y. Kawanishi, K.J. Brewer, Inorg. Chem. 36 (1997) 2861;
(c) J.-D. Lee, L.M. Vrana, E.R. Bullock, K.J. Brewer, Inorg. Chem. 37 (1998) 3575;
(d) C. Ceroni, F. Paolucci, S. Roffia, S. Serroni, S. Campagna, A.J. Bard, Inorg. Chem. 37 (1998) 2829;
(e) A. Klein, V. Kasack, R. Reinhardt, S. Torsten, T. Scheiring, S. Zalis, J. Fiedler, W. Kaim, J. Chem. Soc., Dalton Trans. (1999) 575;

(f) P. Paul, B. Tyagi, A.K. Bilakhia, D. Parthsarthi, E. Suresh, Inorg. Chem. 39 (2000) 14;
(g) G. Albano, P. Belser, C. Dual, Inorg. Chem. 40 (2001) 1408.
[3] (a) M. Ghedini, M. Longeri, F. Neve, J. Chem. Soc., Dalton Trans. (1986) 2669;
(b) M. Ghedini, M. Longeri, F. Neve, A.M.M. Lanfredi, A. Tiripicchio, J. Chem. Soc., Dalton Trans. (1989) 1217;
(c) D.S. Pandey, R.L. Mishra, U.C. Agrawala, Ind. J. Chem. A 30 (1991) 41;
(d) J. Saroja, V. Manivannan, P. Chakraborty, S. Pal, Inorg. Chem. 34 (1995) 3099;
(e) J. Granifo, M.E. Vargas, E.S. Dodsworth, D.H. Farrar, S.S. Fielder, A.B.P. Lever, J. Chem. Soc., Dalton Trans. (1996) 4369;
(f) Z. Xu, S. White, L.K. Thompson, D.O. Miller, M. Ohba, H. Okawa, C. Wilson, J.A.K. Howard, J. Chem. Soc., Dalton Trans. (2000) 1751;
(g) S. Pal, S. Pal, Inorg. Chem. 40 (2001) 4807.
[4] (a) K.E. Erkkila, D.T. Odom, J.K. Barton, Chem. Rev. 99 (1999) 2777;
(b) C.S. Allardyce, P.J. Dyson, Platinum Metals Rev. 45 (2) (2001) 62;
(c) S.R. Korupoju, M. Nagarathinam, P.S. Zacharias, J. Mizuthani, H. Nishihara, Inorg. Chem. 41 (2002) 4099;
(d) H. Chen, J.A. Parkinson, S. Parsons, R.A. Coxall, R.O. Gould, P.J. Sadler, J. Am. Chem. Soc. 124 (2002) 3064;
(e) C.S. Allardyce, P.J. Dyson, D.J. Ellis, S.L. Heath, Chem. Commun. (2002) 1396.
[5] (a) A.M. Pyle, J.K. Barton, in: S.J. Lippard (ed.), Progress in Inorganic Chemistry: Bioinorganic Chemistry, vol. 38, 1990, p. 413;
(b) R.E. Holmlin, P.J. Dandliker, J.K. Barton, Angew. Chem., Int. Ed. Engl. 36 (1997) 2714;
(c) T.W. Hambley, A.R. Jones, Coord. Chem. Rev. 212 (2001) 35;
(d) J.-G. Liu, Q.-L. Zhang, X.-F. Shi, L.-N. Ji, Inorg. Chem. 40 (2001) 5045;
(e) D. Ossipov, P.I. Pradeepkumar, M. Holmer, J. Chattopadhyaya, J. Am. Chem. Soc. 123 (2001) 3551;
(f) Y. Jenkins, A.E. Friedman, N.J. Turro, J.K. Barton, Biochemistry 31 (1992) 10809;
(g) E.M. Proudfoot, J.P. Mackay, P. Karuso, Biochemistry 40 (2001) 4867;
(h) H.D. Stoeffer, N.B. Thornton, S.L. Temkin, K.S. Sxchanze, J. Am. Chem. Soc. 117 (1995) 7119
z(i) A. Wolfe, G.H. Shimer, T. Meehan, Biochemistry 26 (1987) 6392;
(j) M.T. Carter, M. Rodriguez, A.J. Bard, J. Am. Chem. Soc. 111 (1989) 8901;
(k) B.T. Farrer, H.H. Thorp, Inorg. Chem. 39 (2000) 44;
(l) P.J. Carter, C.-C. Cheng, H.H. Thorp, J. Am. Chem. Soc. 120 (1998) 632.
[6] E. Michael, D.A.P. Bundy, Parasitol. Today 13 (1997) 472.
[7] (a) U. Pandya, J.K. Saxena, S.M. Kaul, P.K. Murthy, R.K. Chatterjee, R.P. Tripathi, A.P. Bhaduri, O.P. Shukla,, Med. Sci. Res. 27 (1999) 103;
(b) R.P. Tripathi, S.K. Rastogi, B. Kundu, J.K. Saxena, V.J.M. Reddy, S. Shrivastav, S. Chandra, A.P. Bhaduri, Comb. Chem. Throughput Screen. 4 (2001) 237;
(c) G. Marx, H. Zhou, D.E. Granes, N. Oshroff, Biochemistry 63 (1997) 15884.
[8] D.D. Perrin, W.L.F. Armango, D.R. Perrin, Purification of Laboratory Chemicals, Pergamon, Oxford, V.K., 1986.
[9] (a) W.J. Stratton, D.H. Busch, J. Am. Chem. Soc. 80 (1958) 1286;
(b) M.-A. Haga, K. Koizumi, Inorg. Chim. Acta 104 (1985) 47;
(c) N. Ahmad, J.J. Levison, S.D. Robinson, M.F. Uttley, Inorg. Synth. 15 (1974) 45.
[10] (a) S. Mackay, W. Dong, C. Edwards, A. Henderson, C. Gilmox, N. Stewart, K. Shankland, A. Donald, University of Glasgow, Scotland, 1999;
(b) G.M. Sheldrick, SHELXS-97: Program for Structure Solution and Refinement of Crystal Structure, Gottingen, Germany, 1997;
(c) G.M. Sheldrick, Shelxl-97: program for structure refinement, Gottingen, Germany, 1997;
(d) C.K. Jhonson, ORTEPIII; Report ORNL-5138, Oak Ridge National Laboratory, Oak Ridge, TN, 1976;
(e) PLATON A.L. Spek, Acta Crystallogr., Sect. A 46 (1990) C31.
[11] (a) M.E. Reichmann, S.A. Rice, C.A. Thomas, P. Doty, J. Am. Chem. Soc. 76 (1954) 3074;
(b) J. Marmur, J. Mol. Biol. 3 (1961) 208.
[12] (a) M. Ghedini, M. Longeri, F. Nerve, J. Chem. Soc., Dalton Trans. (1986) 2669;
(b) M. Ghedini, A.M.M. Lanfredi, F. Nerve, A. Tiripicchio, J. Chem. Soc., Chem. Commun. (1987) 847.
[13] (a) D.K. Gupta, O.S. Sisodia, A.N. Sahay, D.S. Pandey, Synth. React. Inorg. Metal Org. Chem. 28 (1998) 355;
(b) M. Chandra, A.N. Sahay, D.S. Pandey, M.C. Puerta, P. Valerga, J. Organometal. Chem. 648 (2002) 39–48.
[14] P. Didier, I. Ortmans, A. Kirsch- De Mesmaeker, R. Watts, J. Inorg. Chem. 34 (1993) 5239.
[15] R.M. Berger, D.D. Elis II, Inorg. Chim. Acta 241 (1996) 1.
[16] B.P. Sullivan, D.J. Salmon, T.J. Meyer, Inorg. Chem. 17 (1978) 3334.
[17] R. Rillema, K.B. Mack, Inorg. Chem. 21 (1982) 3849.
[18] (a) G. Giuffrida, S. Campagna, Coord. Chem. Rev. 135–136 (1994) 517;
(b) P. Ceroni, F. Paolucci, C. Paradisi, A. Juris, S. Roffia, S. Serroni, S. Campagna, A.J. Bard, J. Am. Chem. Soc. 120 (1998) 5480.
[19] P. Ghosh, A. Chakravorty, Inorg. Chem. 36 (1997) 64, and references therein.
[20] (a) M.F. McGuiggan, L.H. Pignolet, Inorg. Chem. 21 (1982) 2523;
(b) A. Sahajpal, S.D. Robinson, M.A. Mazid, M. Motevalli, M.B. Hursthouse, J. Chem. Soc., Dalton Trans. (1990) 2119.
[21] (a) K. Osakada, T. Yamamoto, A. Yamamoto, A. Takenaka, Y. Sasada, Inorg. Chim. Acta 9 (1979) 105;
(b) A.C. Skapski, P.G.H. Throughton, J. Chem. Soc., Chem. Commun. (1968) 1230;
(c) M.R. Churchill, K.M. Keil, F.V. Bright, S. Pandey, G.A. Baker, J.B. Keister, Inorg. Chem. 39 (2000) 5807.
[22] (a) W.S. Sheldrick, H.S. Hagen-Eckhard, S. Heeb, Inorg. Chim. Acta 206 (1993) 15;
(b) H. Brunner, R. Oeschey, B. Nuber, J. Chem. Soc., Dalton Trans. (1996) 1499;
(c) M.E. Gress, C. Creutz, C.O. Quicksall, Inorg. Chem. 20 (1981) 1522;
(d) W. Luginbuhl, P. Zbinden, P.A. Pittet, T. Armbruster, H.-B. Burgi, A.E. Merbach, A. Ludi, Inorg. Chem. 30 (1991) 2350;
(e) A.J. Davenport, D.L. Davies, J. Fawcett, S.A. Garratt, D.R. Russell, J. Chem. Soc., Dalton Trans. (2000) 4432;
(f) D.H. Gibson, J.G. Andino, S. Bhamidi, B.A. Sleadd, M.S. Mashuta, Organometallics 20 (2001) 4956.
[23] (a) W. Saenger, Principles of Nucleic Acid Structures, Springer-Verlag, New York, 1984, p. 132;
(b) L.P.G Wakelin, Med. Res. Rev. 6 (1986) 275;
(c) D. Ranganathan, V. Haridas, R. Gilardi, I.L. Karle, J. Am. Chem. Soc. 120 (1998) 10793;
(d) G.R. Desiraju, T. Steiner, The Weak Hydrogen Bond in Structural Chemistry and Biology, Oxford University Press, Oxford, 1999.

[24] (a) A. Wolfe, G.H. Shimer Jr., T. Meehan, Biochemistry. 26 (1987) 6392;
(b) A.M. Pyle, J.P. Rehmann, R. Meshoyrer, C.V. Kumar, N.J. Turro, J.K. Barton, J. Am. Chem. Soc. 111 (1989) 3051;
(c) A. Ambriose, B.G. Maiya, Inorg. Chem. 39 (2000) 4264, and references therein.

[25] (a) J.K. Barton, Science 233 (1986) 727;
(b) J.K. Barton, J.J. Dannesberg, A.J. Raphel, J. Am. Chem. Soc. 104 (1982) 4967;
(c) J.K. Barton, A.T. Danishefrky, J.M. Goldberg, J. Am. Chem. Soc. 106 (1984) 2172;
(d) A.H.J. Wang, J. Nathans, G.V.D. Marel, J.H.V. Boom, A. Rich, Nature 276 (1978) 471.